# Conceptual Nuclear Design of Innovative Liquid HALEU-loaded Thermal Propulsion Reactor

Reem Alnuaimi[a], and Yonghee Kim[a,*]
[a]*Department of Nuclear & Quantum Engineering, Korea Advanced Institute of Science and Technology (KAIST), 291 Daehak-ro, Yuseong-gu, Daejeon 34141, Republic of Korea*
**Corresponding author: yongheekim@kaist.ac.kr*

***Keywords :*** Nuclear Thermal Rocket (NTR), HTGR, HALEU, Synthetic Diamond (SD)

## 1. Introduction

Future crewed space missions beyond low Earth orbit (LEO) will require advanced propulsion systems that outperform today's chemical engines. The nuclear thermal rocket (NTR) is a promising candidate for this role [1]. NTRs heat a propellant, such as hydrogen, in a nuclear reactor and then expel it through a nozzle to generate thrust, as illustrated in Figure 1. The temperature of the exhaust gas determines the efficiency of rocket engines; the energy of fuel combustion limits chemical engines, while the temperature of the fuel limits nuclear engines. This limitation is due to the maximum temperature that nuclear fuel can withstand, which determines the rate of energy transfer from the fuel to the propellant [3].

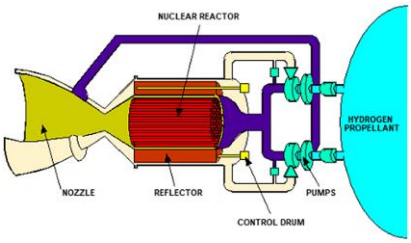


Fig. 1. A typical NTR system [2].

Conventional NTR designs generate heat within the solid fuel, thereby limiting the temperatures that core materials can endure. The use of high-temperature materials is crucial in all rocket engines because it directly affects specific impulse ($I_{sp}$), a key rocket performance parameter. Liquid fuel cores are an advanced approach to bypassing the melting point of uranium-based fuels. This study investigated a preliminary liquid High-Assay Low-Enriched Uranium (HALEU) Nuclear Thermal Rocket core based on a high-temperature gas-cooled reactor (HTGR) concept. The core uses a uranium-manganese (UMn) liquid eutectic metal fuel. It is made up of 94.05% uranium and 5.95% manganese by weight, with 19.75% enrichment of U-235. This design can generate up to 250 MWth and maximize the propellant outlet temperature to above 3000 K.

Unlike solid fuel cores, where fissile products like Xe-135 accumulate and degrade reactivity through neutron absorption, liquid metal fuel systems can effectively remove such byproducts via noble gas diffusion. This is the most advantageous feature of liquid fuel because it minimizes reactivity change during operation and simplifies control. This fuel is liquid at a low melting temperature of 716°C [4] and can operate at high temperatures of up to 3500°C without boiling, allowing the coolant temperature, which also serves as a propellant, to be increased in the NTR without compromising fuel integrity, resulting in improved rocket and nuclear system performance. Furthermore, liquid fuel has the distinct property of having a relatively uniform composition and thus burnup in the axial direction, regardless of the axial power profile, due to fuel element diffusion.

To effectively use thermal neutrons, a moderator material that can withstand high temperatures is required, and there are few options available. To improve thermalization capabilities, this study employs a three-moderator configuration consisting of conventional graphite and BeO, as well as a newly investigated novel Synthetic Diamond (SD) [5]. A recent breakthrough in Synthetic Diamond manufacturing has discovered the possibility of growing diamonds under 1 atm pressure at 1025°C, paving the way for further research, lowering costs, and signaling a significant advancement in diamond synthesis [6]. While SD is still composed of carbon, as graphite, it offers several advantages, such as good stability at high temperatures up to 3500°C, a higher carbon atom density with a theoretical mass density of 3.5 g/cm$^3$ compared to 1.7 g/cm$^3$ of nuclear-grade graphite, and thus superior neutron slowing power and moderating ratio.

## 2. Reactor Concept and Methods

In this study, an active core of 31 fuel elements with a height and diameter of 93.1 cm was designed. To account for the expected neutron leakage from such a compact NTR, a Be reflector with radial and top axial thicknesses of 7 cm and 8 cm is installed. Figure 2 shows detailed cross-sectional views of the core.

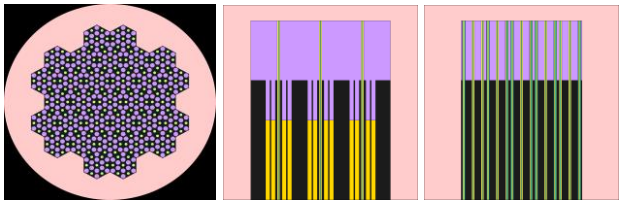

Fig. 2. Cross-sectional views of the NTR core.

The core was optimized to meet several design goals aimed at improving both rocket and nuclear systems performance. For example, the reactor mass was limited to less than 2500 kg to prevent wasting thrust needed to lift the spacecraft. Initially, the coolant outlet temperature, which also serves as the propellant, is set to at least 3000 K to enhance the specific impulse. The reactor is designed to operate primarily in the thermal spectrum to achieve better neutron economy and proliferation resistance. To ensure effective control, the core's excess reactivity limit without SD loading is kept less than 1000 pcm. Additionally, considering that the fuel should remain in the liquid phase, the power profile selected should support efficient heat transfer.

### *2.1 Fuel*

Figure 3a depicts the fuel element's structure as a hexagonal block with a flat-to-flat distance of 13.3 cm. BeO makes up the upper 1/3 blocks of the core, with graphite filling the rest. It can support up to 19 channels. For this work, 7 channels accommodate the fuel, while the remaining 12 positions are filled with BeO and SD moderators, as will be illustrated in the 3-moderator model. Figure 3b and Table I describe the annular fuel channel with inner and outer hydrogen cooling.

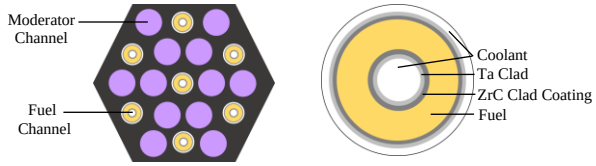


Fig. 3. Structures of a) fuel element and b) fuel channel.

Table I. Fuel channel description

| Layer | Material | Density ($g/cm^3$) | Outer Radius (cm) |
|---|---|---|---|
| Coolant | $H_2$ | 8.40E-5 | 0.118 |
| Inner Clad | Ta | 16.40 | 0.126 |
| Clad Coating | ZrC (100% TD) | 6.730 | 0.131 |
| Fuel | UMn (Liquid) | 15.29 | 0.631 |
| Clad Coating | ZrC (100% TD) | 6.730 | 0.636 |
| Outer Clad | Ta | 16.40 | 0.644 |
| Coolant | $H_2$ | 8.40E-5 | 0.762 |

### *2.2 Moderator*

As previously stated, this design used a 3-moderator model consisting of graphite, BeO, and Synthetic Diamond. The moderator material can be loaded by filling the hexagonal fuel element block, its moderator channels (1.20 cm in radius), or both. Figure 4 demonstrates that there are two options available here: utilize the SD or not. Both options use BeO to fill the blocks and moderator channels in the upper 1/3 of the core region. The lower core, however, is made up of graphite-filled blocks. The top one-third of the moderator channels in the graphite blocks are filled with BeO, and the remainder can be loaded with SD. SD channels are assumed to be partially filled with SD particles, with packing factors of 70%, 75%, 80%, and 85%. To pack the SD into the channels, a vibratory packing technique based on geometrical parameters such as the SD particles' size distribution, shapes, and surface conditions, as well as vibration variables such as frequency, amplitude, and time, could be used [5].

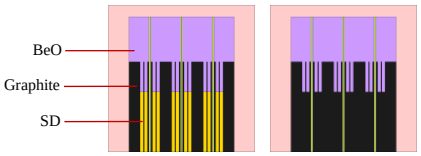


Fig. 4. The 3-moderator model.

### *2.3 Reactor Mass*

Table II shows the detailed mass of the core materials, whereas Table III shows the total mass, which is determined by whether or not it is loaded with SD and the packing factor used.

Table II. Mass of core materials

| Material | Mass (kg) | |
|---|---|---|
| Fuel | U: 347.7115<br>Mn: 21.9976<br>Total: 369.7092 | |
| Graphite | Without SD | 400.1198 |
| | With SD | 281.7417 |
| Be (Reflector) | 866.0991 | |
| Hydrogen (Coolant) | 9.587E-04 | |
| ZrC (Clad Coating) | 3.2548 | |
| Ta (Clad) | 12.6904 | |
| BeO | 511.4228 | |

Table III. SD loading and total mass of the reactor.

| SD Packing Factor | Total SD mass (kg) | Total mass of reactor (kg) |
|---|---|---|
| Without SD | - | 2163.2974 |
| 70% | 170.6037 | 2215.5230 |
| 75% | 182.7897 | 2227.7090 |
| 80% | 194.9757 | 2239.8950 |
| 85% | 207.1616 | 2252.0809 |

## 3. Results and Analysis

Core calculations were performed using the Continuous-Energy Monte Carlo code Serpent 2.20, with 100,000 neutron histories, in 50 inactive and 200 active cycles. Cross-sections of all materials were obtained from the ENDF/B-VIII.0. Due to the library limits, the cross-sections data were evaluated at the maximum temperature of 2500 K. Furthermore, simulations were run with thermal scattering data for the graphite and BeO matrix, as well as the Beryllium reflector. The S(α,β) data were obtained at the maximum temperatures present in the ENDF/B-VII.0 library, 2000 K for graphite and 1200 K for Beryllium

and BeO. Outside the core, vacuum boundary conditions were imposed both radially and axially.

### *3.1 Neutronics*

Table IV shows clearly how SD affects reactivity. To illustrate, the $k_{eff}$ increased from (1.00697 ± 0.00069) without SD to (1.01776 ± 0.00069) with maximum SD loading. This accounts for over a 1052 pcm increase in reactivity. This result is expected given the increase in moderating power caused by the addition of SD channels, which resulted in lower fission reaction rates in the fast region of the spectrum, as shown in Table V and Figure 5. The neutron spectrum observed in the reactor is primarily thermal and epithermal, as illustrated in Figure 6.

Table IV. The multiplication factor of the core

| SD Packing Factor | $k_{eff}$ | $\pm\sigma$ |
|---|---|---|
| Without SD | 1.00697 | 0.00069 |
| 70% | 1.01449 | 0.00064 |
| 75% | 1.01344 | 0.00073 |
| 80% | 1.01553 | 0.00069 |
| 85% | 1.01776 | 0.00069 |

Table V. Energy dependence of fission reaction rate

| SD Packing Factor | Thermal | Epithermal | Fast |
|---|---|---|---|
| Without SD | 46.20692% | 45.87257% | 7.92051% |
| 70% | 46.22991% | 45.94311% | 7.82698% |
| 75% | 46.30570% | 45.89380% | 7.80050% |
| 80% | 46.30679% | 45.91517% | 7.77804% |
| 85% | 46.37333% | 45.87000% | 7.75667% |

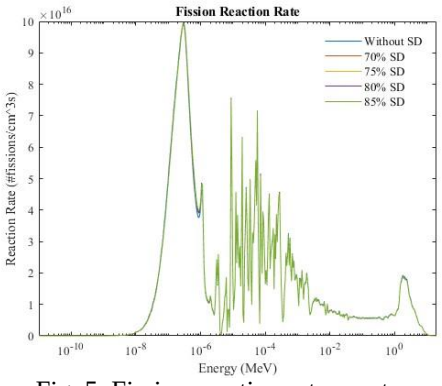


Fig. 5. Fission reaction rate spectrum.

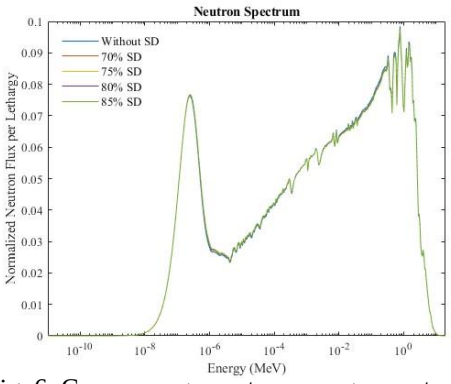


Fig. 6. Core average neutron energy spectrum.

### *3.2 Power Distributions*

This core design is intended to generate 250 MWth. Figure 7 depicts the axial power distribution without SD and at a maximum SD loading of 85%. The addition of SD to the lower region flattens the power peaking factor from 1.87 to 1.75, reducing fission power produced in the BeO region by 4%. The power profile was intentionally designed to keep the UMn fuel in the liquid phase. The radial power distributions for the aforementioned cases are also analyzed for three core regions based on moderator materials: the upper BeO, the middle graphite and BeO, and the lower graphite and SD regions, as illustrated in Figure 8. The majority of fission power is typically generated in the middle region, because, while BeO has greater moderating power than graphite, its absorption cross section is larger. The addition of SD raises the fission power output in the lower region from 18% to 22%. Overall, power profiles are nearly flat, with power peaking factors lower than 1.22.

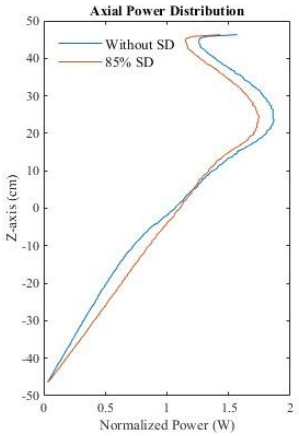


Fig. 7. Normalized axial power distribution.

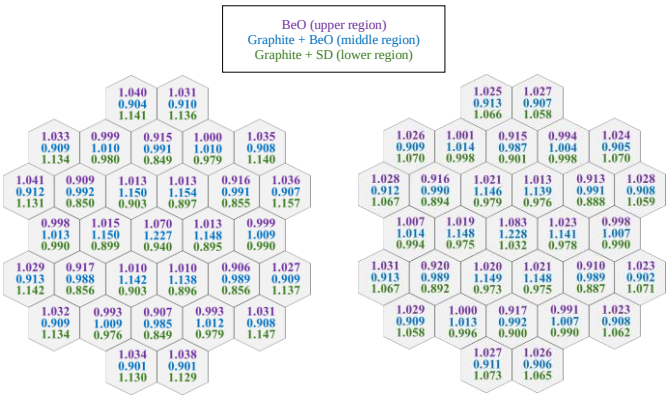


(a) (b)

Fig. 8. Normalized radial power distributions
a) without SD and b) with 85% SD loading.

### *3.3 Reactivity Coefficients*

In terms of preliminary safety analysis, the moderator, fuel, and reflector temperature coefficients were evaluated both without and with 85% SD loading at 2250 K. This calculation was performed without S(α,β) and with 6 million histories over 100 inactive and 500 active cycles, to improve accuracy. Density was adjusted to account for thermal expansion, and because the UMn fuel is liquid, volume shrinkage below the reference temperature of 2500 K was accounted for by filling the upper and lower fuel regions with void when it is denser.

As shown in Table VI, the MTC values are slightly less negative because they incorporate the contributions of competing 3-modreator materials. For example, carbon in graphite and SD behaves generally positively, whereas BeO causes it to behave negatively, as demonstrated by the effect of loading SD into the core. FTC values are strongly negative, giving more assurance that negative feedback will override the MTC's less negative contribution. RTC values are less negative; however, the temperature increase in the reflector region is much smaller and slower than that in the fuel and moderator regions, so it is less concerning.

Table VI. Reactivity Coefficients at 2250 K

| | MTC [pcm/K] | | FTC [pcm/K] | | RTC [pcm/K] | |
|---|---|---|---|---|---|---|
| | NO SD | 85 SD | NO SD | 85 SD | NO SD | 85 SD |
| Reactivity Coefficient | −0.8101 | −0.6040 | −1.9996 | −1.7822 | −0.4776 | −0.5056 |
| ± $\boldsymbol{\sigma}$ | 0.0744 | 0.0741 | 0.0743 | 0.0739 | 0.0745 | 0.0741 |

## 4. Conclusion

In conclusion, this study introduces a new concept for NTR technology, addressing the limitations of solid-core designs through innovative fuel and moderator models. However, to fully assess its potential, it is essential to model the entire reactor system, including the forward region, control mechanisms, and shielding. Additionally, design modifications, comprehensive rocket performance and Multiphysics analyses are necessary to prove the feasibility and safety of the NTR system.

## REFERENCES

[1] P. Venneri and Y. Kim, Advancements in the Development of Low Enriched Uranium Nuclear Thermal Rockets, Energy Procedia, Oct 31-Nov 2, 2016, Tokyo, Japan.
[2] NASA Glenn Research Center, "Nuclear Thermal Propulsion Systems: Typical Components," NASA. [Online]. Available: https://www1.grc.nasa.gov/research-and-engineering/nuclear-thermal-propulsion-systems/typical-components/ . [Accessed: Sept. 2, 2024]
[3] W. Emrich, Principles of Nuclear Rocket Propulsion, Elsevier, Massachusetts, 2023.
[4] A.K. Cea, A. Leenaers, S.V. Berghe and T. Pardoen, Microstructure and calorimetric analysis of the UMn binary system, Journal of Nuclear Materials, Vol.514, pp.380-392, 2019.
[5] R. Alnuaimi, P. Venneri and Y. Kim, Feasibility of Enhancing Neutron Moderation in Nuclear Thermal Propulsion Reactor by Using Synthetic Diamond, Transactions of the American Nuclear Society, Vol. 130, pp. 1076-1079, 2024.
[6] Y. Gong, D. Luo, M. Choe et al., Growth of diamond in liquid metal at 1 atm pressure, Nature, Vol. 629, pp.348–354, 2024.